Branching ratios among three product channels of the dissociative recombination reaction in Ar_2^+

M. Guna, L. Simons, and K. Hardy
Florida International University, University Park, Miami, Florida 33199

J. Peterson
SRI, Menlo Park, California 94025

(Received 13 January 1999)

Measurements of the pressure dependence of the dissociative recombination (DR) reaction transition of Ar_2^+ ($v=0$) to the $3d'[\frac{3}{2}]$ $J=1$, the $4p[\frac{1}{2}]$ $J=1$, and the $4p'[\frac{1}{2}]$ $J=0$ final product states of the argon atom have been done in an argon glow discharge using time-of-flight spectroscopy. The velocity of these final-product-state atoms is close to the most probable velocity ($\approx$750 m/sec) of the argon atoms in the discharge, so that their distributions appear as spikes within the Boltzman distribution. The narrow velocity distributions of these DR product atoms suggests that the velocity of the Ar_2^+ ion parents, which are created by associative ionization reactions, were very subthermal and nearly zero. One collision with an Ar atom would cause the Ar_2^+ ion to gain, on the average, 47% of the velocity of that Ar atom, which would broaden the DR product distribution so that the peak would not be observable. However, if the ion parent dissociates before any collision, the DR distribution will be narrow and thus observable. Determining, experimentally, the pressure at which the narrow peaks broaden and by calculating the collision time corresponding to that pressure, the lifetimes of the DR transitions have been estimated. [S1050-2947(99)01007-0]

PACS number(s): 34.80.Ht

I. INTRODUCTION

The dissociative recombination (DR) reaction in a rare gas involves the capture of a low-energy electron by a rare gas molecular ion, initially produced by associative ionization, the formation of a compound state, and the subsequent dissociation either directly [1] or indirectly [2] into fragments. The typical process for the direct reaction is

$$Ar_2^+ + e^- \Rightarrow Ar_2^{**} \Rightarrow Ar + Ar^{(*)} + E_{ke}. \quad (1)$$

Here Ar_2^{**} represents the dissociative state and the E_{Ke} is the kinetic energy that is released by the reaction. The equation for the indirect reaction is

$$Ar_2^+ + e^- \Rightarrow Ar_{2(n,v)}^{\sharp} \Rightarrow Ar_2^{**} \Rightarrow Ar + Ar^{(*)} + E_{ke}. \quad (2)$$

In the intermediate stage of the indirect reaction, $Ar_{2(n,v)}^{\sharp}$ signifies electron capture into compound resonant Rydberg states, the n represents the different quantum numbers and the v signifies the vibrational level. The $Ar^{(*)}$ product can be in any energy level lower than that of the ion, including the ground state. The other argon atom is normally in its ground state.

In the DR reaction the energy of the final state E_{fs} can be calculated using [3]

$$E_{ke} = E_i - D_0 - E_{fs}, \quad (3)$$

where E_i is the ionization energy of the rare-gas atom, D_0 is the binding energy of the molecular ion, and E_{ke} is the dissociative kinetic energy of the product atoms. Time-of-flight TOF spectroscopy [4] can directly measure the kinetic energy released by the DR reaction of heavy molecular ions such as Ne_2^+ and Ar_2^+, and, therefore, identify the energy state of the final-product atoms. Recent TOF measurements [3] of the DR reaction of Ar_2^+ have revealed very narrow line widths (=25 m/s) for some final-product states from this reaction. In our source, these peaks appear when an external magnetic field is applied to the source. This field also confines the electrons and ions to a narrow region around the axis of the source [5] enhancing reactions such as associative ionization and dissociative recombination in this region.

The width of the velocity distribution of a DR final-product-state atom is broadened by the motion of the parent ionic molecule Ar_2^+, the TOF distribution of the DR atom flux being given by [6]

$$dJ(t) = \frac{c}{t^4} \exp\left\{ \frac{\left[\left(\frac{L}{t}\right) - V_{dr}\right]^2}{V_p^2} \right\} dt. \quad (4)$$

Here dJ is the DR atom flux, C is an arbitrary constant, L is the length of the flight path, V_p is the most probable velocity of the Ar_2^+ ion parents, V_{dr} is the velocity of the DR product in the laboratory system, and t is the TOF. The narrow width of the velocity distributions of some of these DR peaks (which sit atop the broad Boltzmann distribution) indicates that the velocity of the ion parents is subthermal or nearly zero [7]. After only one collision with an Ar atom that has a Maxwellian thermal velocity distribution, the Ar_2^+ ion would gain, on the average, 47% of the velocity of that Ar atom [8]. If this happens, in the case of DR product atoms having velocities (V_{dr}) close to or less than V_p, the most probable velocity of the Maxwellian distribution of the metastable Ar atoms, the DR product distribution will broaden and will not be observable. However, if the parent molecule

is very subthermal and dissociates before any collision, the DR distribution will be narrow and thus observable as in Fig. 1(a). Changing the pressure of the discharge varies the time between collisions. Determining, experimentally, the pressure at which the narrow peaks broaden and calculating the collision time corresponding to that pressure, we are able to estimate the lifetime of these DR transitions. This lifetime is the time between the formation of the Ar_2^+ parent molecule and the time of the dissociative reaction. Since the transition rate is the inverse of the lifetime of the transition, and since the branching ratios are the ratios of the transition rates, this lifetime may be used to calculate the relative branching ratio between transitions whose lifetime has been measured.

II. SPECTRAL WIDTH OF THE DR FINAL-PRODUCT-STATE LINES

Equation (4) gives the DR atom flux dJ from the source [6] seen by the detector, where $V_{\rm dr}$ the velocity of the DR product in the laboratory system, can be calculated from Eq. (3) for each final state in the product atom. Therefore, the DR peak corresponding to a final-product-state atom is broadened by the velocity distribution of the molecular ions that undergo DR. This distribution is characterized by a most probable velocity V_p of the parent molecule before the reaction. The most probable velocity of the Maxwellian distribution V_p, in the case of argon atoms is $\approx$750 m/s. The velocity widths of the ground state and $4s$ DR lines, which predominate the TOF spectrum when no magnetic field is present, were found [6], by fitting the function of the above equation to be 675 ± 125 and 800 ± 200 m/s, respectively. These values agree with the width predicted by Eq. (4) assuming that the parent molecules had Maxwellian velocity distributions characterized by a most probable velocity $v_p \approx 750$ m/s. In recent [6] TOF experiments some DR product atoms in the Boltzmann tail have been observed under various ambient field conditions with widths much narrower than thermal, causing peaks that stand out within the tail, such as those reported here.

K. A. Hardy [7] gives an explanation of the narrow (subthermal) line widths of the slower DR product lines. In a rare gas discharge operating at pressures of several tens of mTorr, the molecular ions that subsequently undergo the DR reaction are formed by the associative ionization reaction. In these reactions, the electron carries off a very small momentum, due to the large mass difference between the atoms and the electron. When the momentum of the ejected electron is ignored and the systems are homonuclear, the conservation of momentum equations can be written in the laboratory reference frame as [Fig. 2(a)]

$$V_1 \sin(\theta) = V_2 \sin(\phi) \tag{5}$$

and

$$2V_{fa} = V_1 \cos(\theta) + V_2 \cos(\phi), \tag{6}$$

which leads to

$$V_{fa} = \frac{V_2 \cos\phi \pm \sqrt{V_2^2 \cos^2\phi - (V_2^2 - V_1^2)}}{2}. \tag{7}$$

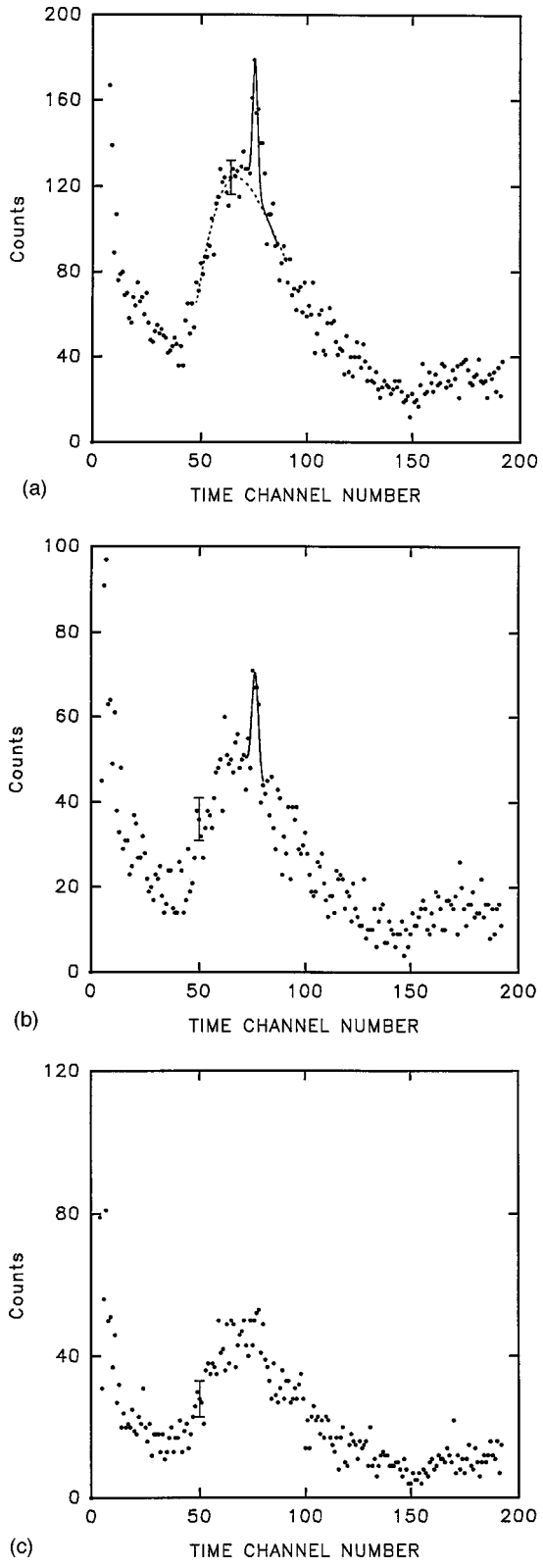

FIG. 1. (a) A time distribution showing the $3d'[\frac{3}{2}]$ $J=1$ final-product-state peak at a pressure of 6 mTorr. The function used to subtract the background is shown in the figure as the dashed line. The points in the neighborhood of the peak were excluded from the fit for the background function. (b) The same final-product-state peak at a discharge pressure of 10 mTorr. (c) At 12 mTorr the peak can no longer be reliably fit to determine the area of the peak. The width of the time channel was 40 μsec.

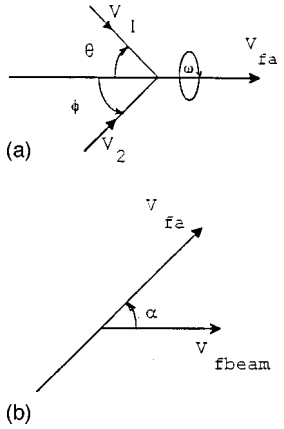

FIG. 2. The kinematics of a collision of two atoms that form a molecular ion Ar_2^+. See Eq. (5) through Eq. (9) in text.

Due to rotational symmetry around the velocity vector of the molecular ion, v_{fa} [Fig. 2(a)], the collision may be treated in two dimensions. The relative probability, $P_r(v_1,v_2)$, of observing this final velocity is proportional to the product of the two Maxwellian probability distributions for each incident atom,

$$P_r(V_1,V_2)\propto V_1^2 e^{-(V_1^2/V_p^2)} V_2^2 e^{-(V_2^2/V_p^2)}. \tag{8}$$

The relative probability, $P_r(v_{fa})$, as a function of final velocity v_{fa} may be determined using Eqs. (7) and (8). The kinematics of the collision are taken into account as there is no contribution to $P_r(v_{fa})$ when the discriminant in Eq. (7) is less than zero. The resulting probability is that of observing the velocity of a molecular ion with the final velocity v_{fa}, along an arbitrary direction (the direction of v_{fa}). Because all directions are equally likely, the component of v_{fa} along the TOF axis is computed by

$$V_{f\text{beam}} = V_{fa}\cos\alpha, \tag{9}$$

where $v_{f\text{beam}}$ is the velocity observed along the time-of-flight axis [Fig. 2(b)]. The relative probability, $P_r(v_{f\text{beam}})$, of observing a particular velocity along the TOF axis is the sum of the probabilities $P_r(v_{fa})$, when the velocities are transformed using Eq. (9).

The numerical modeling of the process revealed that the full width at half maximum of the probability distribution, $P_r(v_{f\text{beam}})$, was in accord with the observed narrow width of the subthermal DR peaks. Moreover, the relative probability of observing the velocity of the molecular ion was found to have a sharp maximum at zero velocity along the TOF axis. The results of these calculations for V_{fa} in the case of no velocity dependence in the associative ionization cross section are shown in Fig. 3(a) and for the case of an associative ionization cross section proportional to $1/V$ in Fig. 3(b). These functions are used in the numerical calculation of the time between collisions.

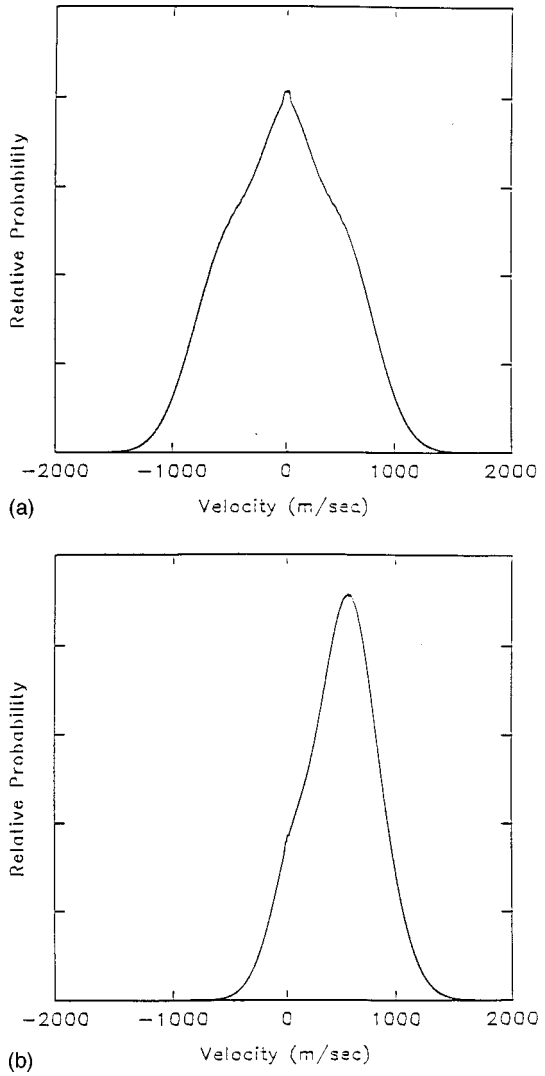

FIG. 3. The numerical functions that show the probability distributions as a function of velocity along the arbitrary axis. These functions are used in the numerical calculation of the time between collisions. (a) shows the distribution assuming no velocity dependence in the associative ionization cross section and (b) shows the distribution assuming a $1/V$ dependence.

III. TIME BETWEEN COLLISIONS

A. Analytical calculation

A good approximation to the collision time between a molecular ion Ar_2^+ and an Ar atom can be calculated analytically using the hard-sphere model by considering that in the discharge the two kinds of particles have Maxwellian velocity distributions. In the following expressions, the subscript ''*i*'' refers to the Ar_2^+ ions and the subscript ''*a*'' refers to the Ar atoms, unless otherwise noted.

The number of the argon ions, Ar_2^+, which have a speed between v and $v+dv$, is

$$n' = N' \frac{4}{\beta^3\sqrt{\pi}} V^2 e^{-V^2/\beta^2} dV, \tag{10}$$

where N' is the total number of argon ions, Ar_2^+ in the mixture of gases, and β is the most probable speed given by

$$\beta = \sqrt{\frac{2kT_i}{m_i}}. \tag{11}$$

The number of argon atoms whose speed relative to the Ar_2^+ ions is between V_r and V_r+dV_r is

$$n=N\frac{V_r}{\alpha V\sqrt{\pi}}[e^{-(V_r-V)^2/\alpha^2}-e^{-(V_r+V^2)^2/\alpha^2}]dV_r, \quad (12)$$

where N is the total number of Ar atoms and the most probable speed α is

$$\alpha=\sqrt{\frac{2kT_a}{m_a}}. \quad (13)$$

The number of pairs, which approach within distance s in unit time, is

$$nn'\pi V_r s^2=NN'4s^2\frac{V_r^2}{\alpha\beta^3}[e^{-(V_r-V)^2/\alpha^2} - e^{-(V_r+V)^2/\alpha^2}]e^{-V^2/\beta^2}dV_r dV. \quad (14)$$

Integrating with respect to V,

$$\left[\int_0^\infty NN'4s^2\frac{V_r^2}{\alpha\beta^2}(e^{-(V_r-V)^2/\alpha^2} - e^{(V_r+V)^2/\alpha^2})e^{-V^2/\beta^2}dV\right]dV_r \quad (15)$$

gives

$$NN'4\sqrt{\pi}s^2\frac{V_r^3}{(\alpha^2+\beta^2)^{3/2}}e^{-V_r^2/(\alpha^2+\beta^2)}dV_r. \quad (16)$$

Integrating this from $V_r=0$ to $V_r=\infty$,

$$\int_0^\infty NN'4\sqrt{\pi}s^2\frac{V_r^3}{(\alpha^2+\beta^2)^{\frac{3}{2}}}e^{-V_r^2/(\alpha^2+\beta^2)}dV_r \quad (17)$$

gives the number of collisions in unit time that take place in unit volume between particles of different kinds. The result is

$$2NN'\sqrt{\pi}\sqrt{\alpha^2+\beta^2}s_{ai}^2, \quad (18)$$

s_{ai} being the distance of centers of collision.

The number of collisions between two Ar atoms is

$$2(N')^2\sqrt{\pi}\sqrt{2\alpha^2}s_a^2 \quad (19)$$

and for the Ar_2^+ ions it is

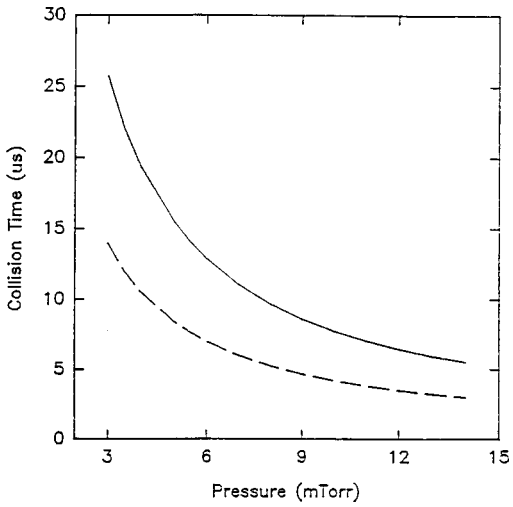

FIG. 4. Results of the analytical calculation of the time between collisions for the Maxwellian distribution is shown as a solid line. The results of the numerical calculation for the associative ionization distribution shown in Fig. 3 are shown as a dotted line. The solid line is Eq. (27) and the dashed line is Eq. (28) (see text).

$$2N^2\sqrt{\pi}\sqrt{2\beta^2}s_i^2. \quad (20)$$

If l_a and l_i are the mean distances traveled by the atoms and the ions, respectively, between each collision, then

$$\frac{1}{l_a}=\pi N\sqrt{2}s_a^2+\pi N'\sqrt{\frac{(\alpha^2+\beta^2)}{\alpha^2}}s_{ai}^2, \quad (21)$$

$$\frac{1}{l_i}=\pi N'\sqrt{2}s_i^2+\pi N\sqrt{\frac{(\alpha^2+\beta^2)}{\beta^2}}s_{ai}^2. \quad (22)$$

If $T_a=T_i=T$, then Eqs. (21) and (22) reduce to [7]

$$\frac{1}{l_n}=\pi\sum_o n_o s_{no}^2\sqrt{1+\frac{m_n}{m_o}}, \quad (23)$$

where l_n is the mean-free path of either an ion (i) or an atom (a) between collisions with the other ''o'' kind of particle in a mixture of gases, m_o is the mass of the other (''o'') type particle, and s_{no} the distance between the centers of collisions, which is given by

$$S_{no}=(d_n+d_o)/2. \quad (24)$$

TABLE I. Velocity calculation for Argon.

Final state	$3d'\ [\frac{3}{2}]\ J=1$	$4p'\ [\frac{1}{2}]\ J=0$	$4p\ [\frac{1}{2}]\ J=1$
Ionization energy E	15.76 eV	15.76 eV	15.76 eV
Binding energy, Ar_2^+ D_0	1.23 eV	1.23 eV	1.23 eV
Energy available $E_a=E-D_0$	14.47 eV	14.47 eV	14.47 eV
Final-state energy E_{fs}	14.31 eV	13.48 eV	12.91 eV
Dissociative KE E_{KE}	.16 eV	.99 eV	1.56 eV
Velocity $V=E_{KE}/M^{1/2}$	737 m/s	1587 m/s	1974 m/s

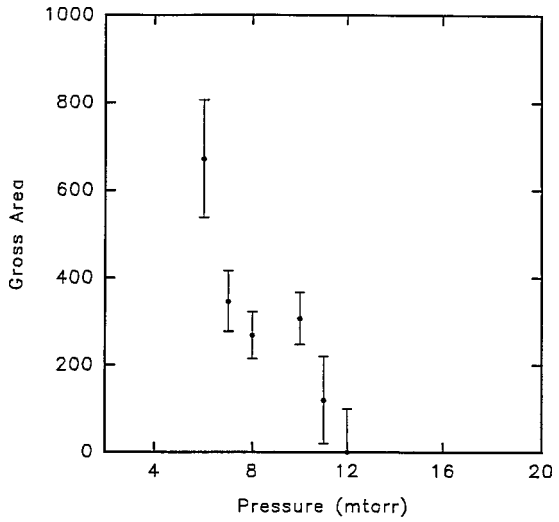

FIG. 5. The area of the $3d'[\frac{3}{2}]$ $J=1$ final-product-state peak as a function of pressure.

In Eq. (24) d_n is the diameter of the ion or atom, and d_o is the diameter of the other type of particle. In our source $N_{\mathrm{Ar2+}} \ll N_{\mathrm{Ar}}$; therefore,

$$\tau_{a\to i}=\frac{1}{\pi N_{\mathrm{Ar}}\sqrt{V_a^2+V_i^2}s_{ai}^2}, \tag{25}$$

where V_i and V_a are the mean speeds of Ar_2^+ ions and Ar atoms, respectively. Since $V_i \ll V_a$ the upper limit of the collision time is

$$\tau_{a\to i}=\frac{1}{\pi N_{\mathrm{Ar}}V_a s_{ai}^2}, \tag{26}$$

which in our experiment leads to the expression

$$\tau_{a\to i}=\frac{77.1\ \mu\mathrm{sec}}{p}, \tag{27}$$

where P is the discharge pressure in mtorr. The calculation above assumes that the atoms and molecular ions had Maxwellian velocity distributions. This function is plotted for the range of pressures used in this measurement in Fig. 4.

B. Numerical calculation

It has been shown [7] that the velocity distribution of the molecular ions, when formed by associative ionization, is far from a Maxwellian distribution. The probability distributions along an arbitrary direction in the source are shown in Fig. 3(a) when the associative ionization cross section does not depend on velocity and in Fig. 3(b) when the cross section has a $1/V_{\mathrm{rel}}$ dependence, which is closer to reality [9]. These distributions are used in place of the function of Eq. (10). The numerical result was used in Eq. (14). For convenience, the integration in Eq. (17) was done for each n', V pair, and then the integration in Eq. (15) was done numerically. This numerical result replaces Eq. (18). The result of the numerical calculations are shown in Fig. 4. There was no significant difference in the dependence of the collision time on pressure between the two speed distributions used for the mo-

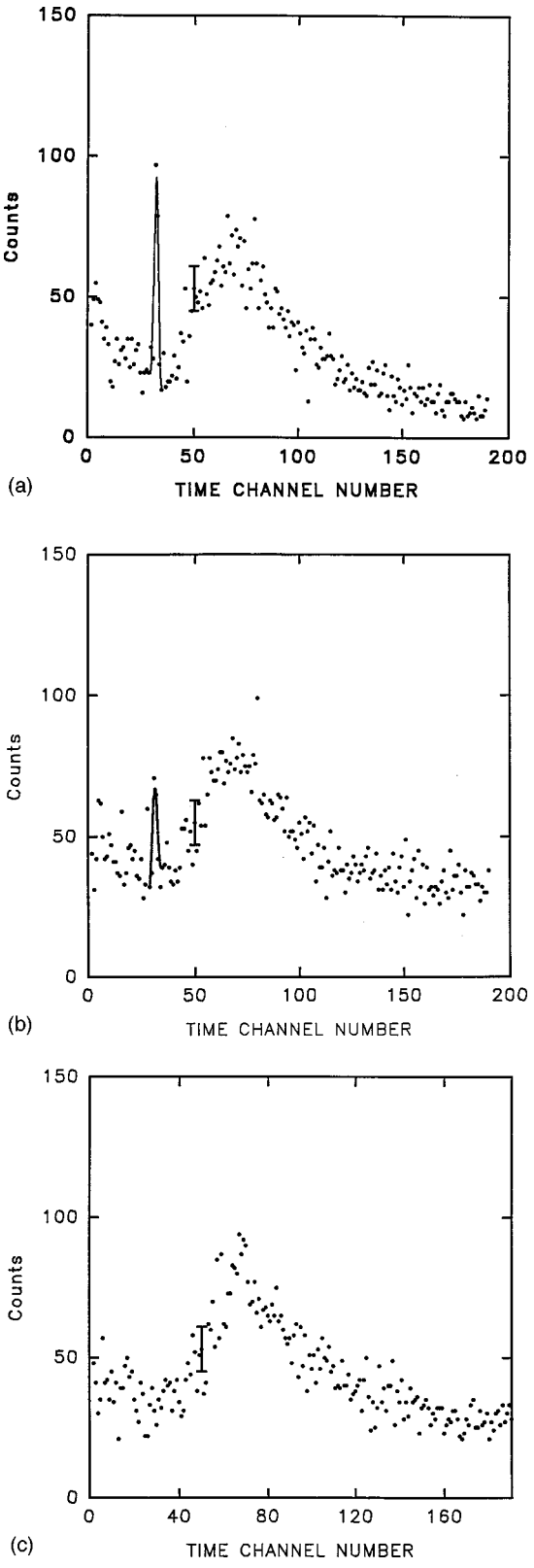

FIG. 6. The $4p'[\frac{1}{2}]$ $J=0$ final-product-state peak as a function of pressure. The spectra were taken with pressures of (a) 8 mTorr, (b) 13 mTorr, and (c) 14 mTorr. At 14 mTorr the peak has been broadened and is no longer distinguishable from the background. The width of the time channel was 40 μsec.

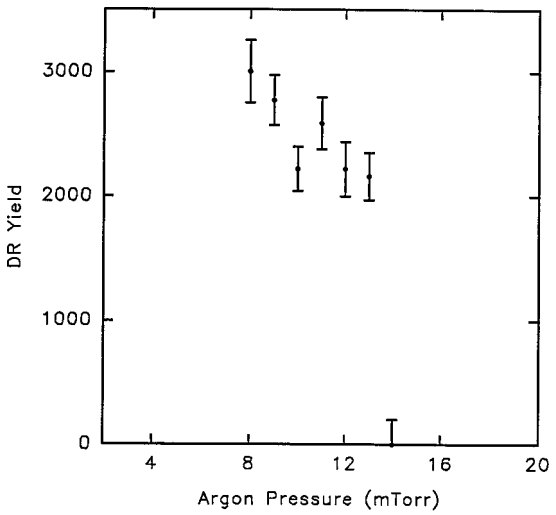

FIG. 7. The yield of the $4p'[\frac{1}{2}]\ J=0$ final-product-state peak as a function of pressure.

lecular ions. The numerical calculation using the associative ionization velocity distribution leads to the expression,

$$\tau_{a\to i}=\frac{42.0\ \mu\text{sec}}{p}. \tag{28}$$

This function is plotted as a dashed line in Fig. 4.

IV. FINAL-PRODUCT-STATE IDENTIFICATION

The DR reaction, such as Eq. (1) or Eq. (2), can be written in simplified form as

$$\mathrm{Ar}_2^{+}+e^{-}\Rightarrow \mathrm{Ar}^{*}+\mathrm{Ar}+E_{\mathrm{ke}}, \tag{29}$$

where dissociative kinetic energy, E_{ke} is released. Once the dissociative kinetic energy of the reaction is obtained experimentally, the final state can be identified since the DR to each electronic state releases a known amount of energy. By knowing the TOF, the velocity can be obtained. With this velocity and the mass of the atom (Argon: 39.9 amu), the kinetic energy released per atom can be calculated using $\frac{1}{2}$ Mv^2. With the ionization energy of the rare-gas atom E_i, the dissociation energy of the molecular ion D_0, the energy available for the dissociative recombination reaction can be determined. Subtracting the energy of the electronic state of the final product from the energy available will give the dissociative kinetic energy released E_{ke} [Eq. (3)],

$$E_{\mathrm{ke}}=E_i-D_0-E_{\mathrm{fs}}.$$

This is the energy for the two particles of the diatomic ion. The Ar_2^{+} ion core is homonuclear so the kinetic is split evenly between the two products. Therefore, half of the E_{ke} is the kinetic energy $\frac{1}{2}Mv^2$ for one of the final-product atoms. Expected velocities and energies, once calculated, can then be compared with the energies obtained from published energy level diagrams [10] to identify the states.

The calculations for the Ar_2^{+} transitions to the $3d'[\frac{3}{2}]J=1$, $4p[\frac{1}{2}]J=1$, and the $4p'[\frac{1}{2}]J=0$ states of the final-product atom are shown in Table I.

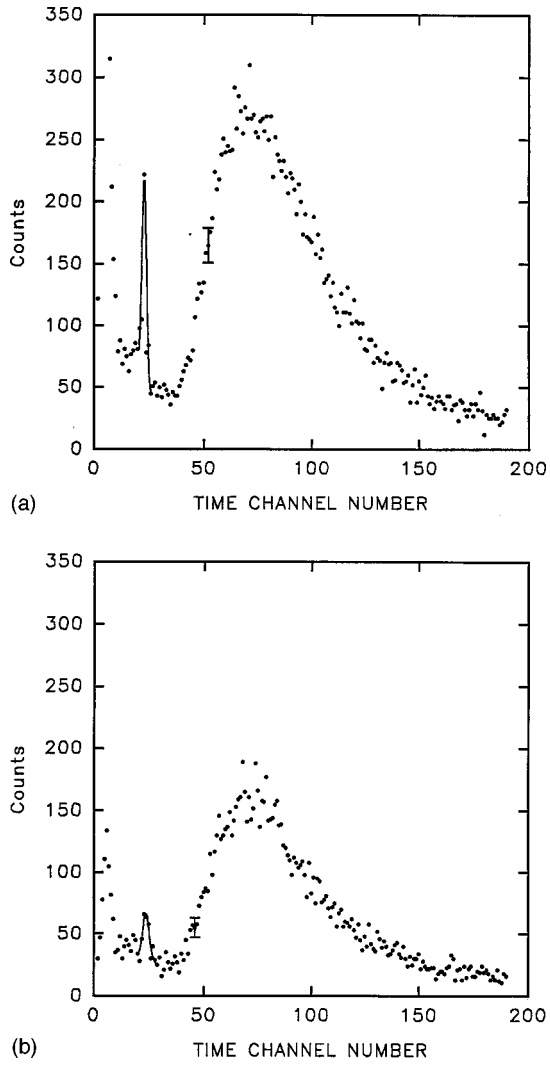

FIG. 8. The $4p[\frac{1}{2}]\ J=1$ final-product-state peak at pressures of (a) 7 mTorr and (b) 18 mTorr. The width of the time channel was 40 μsec.

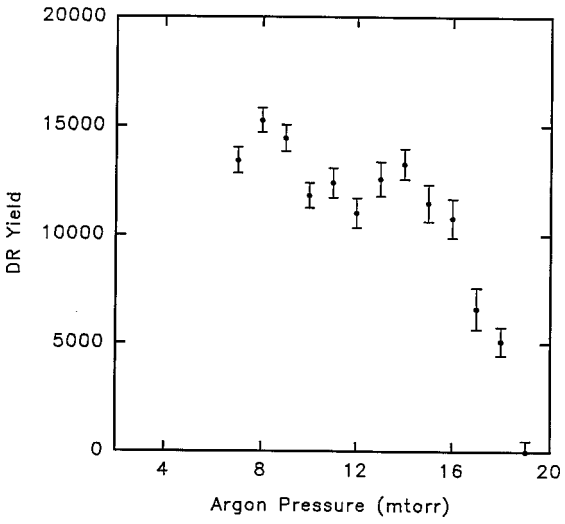

FIG. 9. The yield of the $4p[\frac{1}{2}]\ J=1$ final-product-state peak as a function of pressure.

V. EXPERIMENTAL DATA

In our time-of-flight apparatus the reactions occur in a glow discharge immersed in a uniform but variable magnetic field. The reaction products and metastable atoms escape through a pinhole and are detected by measuring Auger electrons ejected from a gold-plated mirror and collected by a Channeltron electron multiplier. A set of sweep plates removes all charged particles and Rydberg-state atoms from the beam. Using 200 channels on a nultichannel scaler with a time per channel of 40 μsecs and a flight-path length of 1.824 m the velocity resolution at the low-velocity end of the spectrum is 8 m/s and the energy resolution is 1.6×10^{-5} eV. A detailed discussion of the apparatus will be found elsewhere [3–7].

The dissociative recombination products can be identified by their characteristic shape, which is Gaussian in velocity space.

$$dJ(t) = \frac{C}{t^4} \exp\left\{ \frac{\left[\left(\frac{L}{t}\right) - V_{\mathrm{DR}}\right]^2}{V_p^2} \right\} dt. \tag{4}$$

The data were fitted to the function of Eq. (4) where V_{DR} is determined from the known release of dissociative kinetic energy E_{KE}, which depends on the final-product state of the DR reaction. Here L is the length of the flight path and t is the time of flight. There are two free parameters in the fit, the amplitude, and the width. All the other variables are determined by the assumed final-product state. The conclusive identification of the state is made by identifying the state that gives a minimum in the χ^2 of the fit.

The thermal Ar* atoms that comprise the Maxwellian distribution are formed by the primary fast electrons in the source. This distribution has been fitted with the following formula (in the case of the $3d'[\frac{3}{2}]J=1$ state):

$$f(t) = \frac{C}{t^5}\left[-\frac{5}{2}\left(\frac{t_p}{t}\right)^2 \right], \tag{30}$$

where t_p is the most probable time and C is a constant. The background function used for the $4p'$ and $4p$ final products was a straight line, parameters of which were determined by the best χ^2.

The yield of the $3d'[\frac{3}{2}]J=1$, the $4p'[\frac{1}{2}]J=0$, and the $4p[\frac{1}{2}]J=1$ final product state atoms (shown in Figs. 1, 8, and 9) from the dissociative recombination of Ar_2^+ was measured as a function of the pressure in an argon glow discharge at pressures between 6 and 20 mTorr. The source conditions were a discharge voltage of 50 V, a discharge current of 300 mA, and a magnetic field of 70 G. The only variable parameter was the source pressure. Figure 1(a), 1(b), and 1(c) show the DR reaction products to $3d'[\frac{3}{2}]J=1$ final-product state at pressures of 6 mTorr [Fig. 1(a)], 10 mTorr [Fig. 1(b)], and 12 MTorr [Fig. 1(c)]. As can be seen in Fig. 1, increasing the pressure in the discharge causes a decrease in the yield of the observable DR final-product-state atoms. At a pressure of 12 mTorr the DR peak could no longer be clearly distinguished from the background Boltzman distribution of metastable Ar* atoms. The area of the DR final-product-state peak shown in Fig. 1 at channel 74 is plotted as a function of pressure in Fig. 5.

The yield of the $4p'[\frac{1}{2}]J=0$ final-product state was measured as a function of pressure at pressures between 8 and 14 mTorr. This data is shown in Fig. 6. At 14 mTorr the peak in channel 32 was broadened to the extent that it could no longer be observed above the background. The yield as a function of pressure for this DR transition is shown in Fig. 7. The yield of the $4p[\frac{1}{2}]J=1$ final-product state is shown in Fig. 8 at channel 23 at pressures of up to 20 mTorr. The yield as a function of pressure is shown in Fig. 9.

Using a pressure of 12 mTorr and the expression from Eq. (28), $\tau = 42.0\ \mu$sec/P, which assumes the calculated velocity distributions for the molecular ions from associative ionization and uses the numerical calculation for the time between collisions, the time of the DR transition from Ar_2^+ to the $3d'[\frac{3}{2}]J=1$ final-product state in the argon atom is $t = 4 \pm .2\ \mu$sec. The same analysis is applied to the transitions to the $4p'$ and $4p$ final-product-state peaks and we find that the lifetime of the $4p'[\frac{1}{2}]J=0$ is $t = 2.2 \pm .1\ \mu$sec and for the DR transition to the $4p[\frac{1}{2}]J=1$ state the lifetime is $t = 3 \pm .2\ \mu$sec. The transition rate is inversely proportional to the lifetime of the transition, so the relative transition rates, and, therefore, the branching ratios may be calculated from these times. We chose to calculate the branching ratios relative to the slowest of the three transitions and find that the branching ratio (BR) $3d'/4p$ is $.75 \pm .07$ and BR $3d'/4p'$ is $.55 \pm .07$.

VI. CONCLUSION

The yields of the $3d'[\frac{3}{2}]J=1$, the $4p[\frac{1}{2}]J=1$, and the $4p'[\frac{1}{2}]J=0$ final-product-state atoms from the dissociative recombination of Ar_2^+ have been measured as functions of the pressure in an argon glow discharge. The source conditions were a discharge voltage of 50 V, a discharge current of 300 mA, and a magnetic field of 70 G. The only variable parameter was the source pressure. Experimental evidence [6] indicates that the velocity distributions of the molecular ions formed by associative ionization are not Maxwellian and very narrow until they undergo a collision with the ambient gas. We have used the pressure dependence of the yield of these DR transitions to determine the lifetimes of the transitions. We conclude that the lifetimes of the molecular ions produced from associative ionization when these ions undergo a DR transition from Ar_2^+ to the $3d'[\frac{3}{2}]J=1$ final-product state have been determined to be $t = 4 \pm .2\ \mu$sec, to the $4p[\frac{1}{2}]J=1$ final-product state is $3 \pm .2\ \mu$sec, and to the $4p'[\frac{1}{2}]J=0$ final-product state the time is $2.2 \pm .1\ \mu$sec. These lifetimes can be used to determine the branching ratios to the $4p$ and $4p'$ relative to the $3d'$ state. They are (BR) $4p/3d' = 1.33 \pm .13$ and (BR) $4p'/3d' = 1.82 \pm .23$. The inverse lifetimes t^{-1} are products of the rate constant times the electron density that is undetermined but the same in all these measurements. The rate constants and their ratios can be calculated and thus these ratios are tests for future theory.

[1] J. N. Bardsley, J. Phys. B **1**, 349 (1968).
[2] A. P. Hickman, *Resonance in Dissociative Recombination of Electrons with* H_2^+, *Dissociative Recombination: Theory, Experiment, and Applications* (World Scientific, Singapore, 1989).
[3] G. B. Ramos, M. Schlamkowitz, J. W. Sheldon, K. A. Hardy, and J. R. Peterson, Phys. Rev. A **52**, 4556 (1995).
[4] K. A. Hardy and J. W. Sheldon, Rev. Sci. Instrum. **52**, 1802 (1981).
[5] A. Barrios, G. B. Ramos, K. A. Hardy, and J. W. Sheldon, J. Appl. Phys. **76**, 728 (1994).
[6] K. A. Hardy and J. W. Sheldon, Phys. Rev. A **51**, 2945 (1995).
[7] K. A. Hardy, Phys. Rev. A **58**, 1256 (1998).
[8] A. M. Howatson, *An Introduction to Gas Discharges* (Pergamon, Elmsford, NY, 1965).
[9] J. Weiner, F. Masnou-Seeuw, and A. Giusti-Suzor, *Associative Ionization: Experiments, Potentials, and Dynamics: Advances in Atomic, Molecular, and Optical Physics* (Academic, New York, 1989), Vol. 26.
[10] C. E. Moore, *Atomic Energy Levels*, Natl. Bur. Stand. (U.S.) Circ. No. 35 (U.S. GPO, Washington, DC, 1949), Vol. 1.